2004

Spectrum and Transition Rates of the XX Chain Analyzed via Bethe Ansatz

Daniel Biegel

Michael Karbach
University of Rhode Island

See next page for additional authors

Citation/Publisher Attribution
D. Biegel, M. Karbach, G. Müller, and K. Wiele. Spectrum and transition rates of the XX chain analyzed via Bethe ansatz. Physical Review B, 69 (2004), 174404, pp. 1-9.
Available at: http://dx.doi.org/10.1103/PhysRevB.69.174404

Spectrum and transition rates of the *XX* chain analyzed via Bethe ansatz

Daniel Biegel,[1] Michael Karbach,[1,2] Gerhard Müller,[2] and Klaus Wiele[1]
[1]*Bergische Universität Wuppertal, Fachbereich Naturwissenschaften, Physik, D-42097 Wuppertal, Germany*
[2]*Department of Physics, University of Rhode Island, Kingston, Rhode Island 02881-0817, USA*
(Received 8 September 2003; published 6 May 2004)

As part of a study that investigates the dynamics of the $s=\frac{1}{2}$ *XXZ* model in the planar regime $|\Delta|<1$, we discuss the singular nature of the Bethe ansatz equations for the case $\Delta=0$ (*XX* model). We identify the general structure of the Bethe ansatz solutions for the entire *XX* spectrum, which include states with real and complex magnon momenta. We discuss the relation between the spinon or magnon quasiparticles (Bethe ansatz) and the lattice fermions (Jordan-Wigner representation). We present determinantal expressions for transition rates of spin-fluctuation operators between Bethe wave functions and reduce them to product expressions. We apply the formulas to two-spinon transition rates for chains with up to $N=4096$ sites.

DOI: 10.1103/PhysRevB.69.174404 PACS number(s): 75.10.−b

I. INTRODUCTION

The key to a meaningful interpretation of experimental or computational data for the low-temperature dynamics of quantum many-body systems is a thorough understanding of the nature of the physical vacuum and the dynamically relevant collective excitations including their quasiparticle composition. In completely integrable systems, the quasiparticle configurations that produce particular collective excitations can be investigated closely. The identity of the former is preserved by conservation laws notwithstanding their mutual interaction.[1,2] Integrable Hamiltonians that depend on continuous parameters make it possible to observe how the physical vacuum transforms gradually and, occasionally, changes abruptly across a quantum phase transition. Along the way, the configurations of quasiparticles in the collective excitations are subject to change as well.

Recently, we investigated the metamorphosis of the physical vacuum and the dynamically relevant quasiparticles (magnons, spinons, ψ, ψ^*) of the one-dimensional(1D) $s=\frac{1}{2}$ Heisenberg antiferromagnet (*XXX* model) by varying the (integrability preserving) external magnetic field.[3,4] Introducing instead a uniaxial exchange anisotropy also preserves integrability. The parameter Δ, which controls the anisotropy in the 1D $s=\frac{1}{2}$ *XXZ* model,[5]

$$H \doteq \sum_{n=1}^{N} \{S_n^x S_{n+1}^x + S_n^y S_{n+1}^y + \Delta S_n^z S_{n+1}^z\} - \Delta \frac{N}{4}, \quad (1.1)$$

affects the physical vacuum and the quasiparticle configurations differently. In both situations, the Bethe ansatz is an ideal framework for studying quasiparticles, their transformations, and their interactions.

The main focus in this paper is on a technical point of considerable importance in the study of the *XXZ* model, namely, the identification of the general structure of the Bethe ansatz solutions of all eigenstates for the case $\Delta=0$ (*XX* model). This will facilitate tracking all *XXZ* Bethe ansatz solutions across the planar regime, $|\Delta|<1$.

At $\Delta=0$ all states can be characterized as noninteracting composites of fermions. Understanding the relationship between the magnon, spinon, and lattice fermion quasiparticles is important for the interpretation of the excitation spectrum via dynamical probes as realized experimentally or computationally. Furthermore, recent advances in calculating transition rates via Bethe ansatz[6–10] offer opportunities to extend the list of exact results for dynamical properties of the *XX* chain.

In Sec. II we analyze the singularities of the *XXZ* Bethe ansatz equations for $\Delta\to 0$. In Sec. III we discuss the mapping between the spinon and fermion compositions of the *XX* spectrum. The two-spinon spectrum of the planar *XXZ* model including the *XX* limit is discussed in Sec. IV. In Sec. V transition rate formulas for the *XXZ* model are introduced and further processed for the *XX* limit. The two-spinon part of the dynamic spin structure factor $S_{-+}(q,\omega)$ is discussed in Sec. VI.

II. BETHE ANSATZ EQUATIONS

We consider Hamiltonian (1.1) for even N and periodic boundary conditions over the range $0\leqslant\Delta\leqslant 1$ of the anisotropy parameter. In the invariant subspace with z component of the total spin $S_T^z=N/2-r$, all eigenstates are represented by r interacting magnons. The magnon momenta k_i are conserved in the scattering processes and are determined by the Bethe ansatz equations:[11]

$$e^{iNk_i}=\prod_{j\neq i}^{r}\left[-\frac{1+e^{i(k_i+k_j)}-2\Delta e^{ik_i}}{1+e^{i(k_i+k_j)}-2\Delta e^{ik_j}}\right], \quad i=1,\ldots,r. \quad (2.1)$$

The energy and wave number of any such r-magnon state depend on the magnon momenta alone:

$$E=\sum_{i=1}^{r}(\cos k_i-\Delta), \quad k=\sum_{i=1}^{r} k_i. \quad (2.2)$$

At first glance it looks as if Eqs. (2.1) are drastically simplified in the limit $\Delta\to 0$ with all magnon momenta restricted to solutions of $e^{iNk_i}=(-1)^{r-1}$. However, a closer look reveals that magnon pairs with momenta $k_i+k_j\to\pi$ for $\Delta\to 0$ are a common occurrence. This opens the door to nontrivial real and complex solutions of Eqs. (2.1). The singular

behavior is related to level degeneracies. Such level crossings, which also occur at other values of Δ, have been traced back to a realization of the sl_2 loop algebra symmetry at $\Delta=(q+q^{-1})/2\neq\pm 1$ with $q^{2N}=1$ for $N\geqslant 2$.[12–14]

In the following, we use the anisotropy parameter

$$\gamma \doteq \arccos\Delta \quad (0\leqslant\gamma\leqslant\pi/2) \tag{2.3}$$

and transform the magnon momenta into the rapidities,[15]

$$y_i \doteq \tan\frac{\gamma}{2}\cot\frac{k_i}{2}, \quad i=1,\ldots,r. \tag{2.4}$$

The Bethe ansatz equations (2.1) thus become

$$\left(\frac{c_2 y_i+\mathrm{i}}{c_2 y_i-\mathrm{i}}\right)^N=\prod_{j\neq i}^{r}\frac{c_1(y_i-y_j)+i(1-y_i y_j)}{c_1(y_i-y_j)-i(1-y_i y_j)} \tag{2.5}$$

for $i=1,\ldots,r$, with $c_1\doteq\cot\gamma$ and $c_2\doteq\cot(\gamma/2)$. Taking the logarithm yields

$$N\phi(c_2 y_i)=2\pi I_i+\sum_{j\neq i}^{r}\phi\left(c_1\frac{y_i-y_j}{1-y_i y_j}\right), \quad i=1,\ldots,r, \tag{2.6}$$

with $\phi(x)\doteq 2\arctan(x)$. Expressions (2.2) for energy and wave number now read

$$E=-\frac{2}{c_2^{-1}+c_2}\sum_{i=1}^{r}\frac{y_i^{-1}-y_i}{(c_2 y_i)^{-1}+c_2 y_i}, \tag{2.7}$$

$$k=\pi r-\frac{2\pi}{N}\sum_{i=1}^{r} I_i. \tag{2.8}$$

The trigonometric Bethe ansatz equations (2.6) have the advantage that each solution is characterized by a set of (integer or half-integer) Bethe quantum numbers I_i. These discriminating markers are used to count and classify the solutions and are essential for numerical algorithms designed to find solutions.

A. *XX* limit

Here we describe the general structure of the solutions of the Bethe ansatz equations (2.6) in the limit $\Delta\to 0$, implying $c_1\to 0$ and $c_2\to 1$. There exist regular solutions and singular solutions. The latter are characterized by the occurrence of pairs of rapidities y_i, y_i' with the property $y_i y_i'=1$. For any such *critical pair*, the argument of ϕ on the right-hand side of Eqs. (2.6) is indeterminate and must, therefore, be treated as a limit process. We shall see that some limiting singular solutions are real while others are complex. An important fact is that the simplified structure of the Bethe ansatz equations at $\Delta=0$ affords a universal treatment of the singularities for arbitrary N. Knowing the general structure of all Bethe ansatz solutions for this case is a useful reference point for studies which pursue related goals for the XXX and XXZ models.[16–21]

In the absence of any critical pair of rapidities, Eqs. (2.6) decouple and yield the solutions

$$y_i=\tan\left(\frac{\pi I_i}{N}\right)\Leftrightarrow k_i=\pi-\frac{2\pi}{N}I_i \tag{2.9}$$

for $i=1,\ldots,r$, which are all real. The energy of any such regular state is

$$E=-\sum_{i=1}^{r}\frac{y_i^{-1}-y_i}{y_i^{-1}+y_i}=\sum_{i=1}^{r}\cos k_i. \tag{2.10}$$

B. Real critical pairs

Now let us assume that among the set of rapidities $y_1,\ldots,y_r$, there is one critical pair,

$$y_j^0 y_{j*}^0=1\Leftrightarrow k_j+k_{j*}=\pi(\mathrm{mod}\,2\pi), \tag{2.11}$$

and that it is a real pair. Substituting the ansatz

$$y_i=y_i^0+c_1\delta_i, \quad i=1,\ldots,r, \tag{2.12}$$

into Eqs. (2.6) and taking the limit $c_1\to 0$ then yields the noncritical and critical rapidities from successive orders in a c_1 expansion. The noncritical rapidities y_i, $i\neq j,j*$, are given by Eqs. (2.9) as in regular solutions. The c_1 expansion of Eqs. (2.6) leads to the following equation determining the critical rapidities y_j^0, y_{j*}^0:

$$\phi(y_j^-)=\frac{2}{N}\phi\left(\left[\frac{\sigma_j y_j^-}{1-\xi_j}\right]^{\sigma_j}\right). \tag{2.13}$$

Here we have introduced $y_j^{\pm}=\frac{1}{2}(y_j^0\pm y_{j*}^0)$ and we use

$$\xi_j\doteq\frac{2}{N}\sum_{i\neq j,j*}^{r}\frac{y_j^+-\sin k_i}{(y_j^+)^{-1}-\sin k_i}, \tag{2.14}$$

$$\mathrm{sgn}\left(\frac{y_j^+}{\xi_j}\right)=-\frac{2}{N}(I_j+I_{j*}), \quad \sigma_j\doteq(-1)^{I_j-I_{j*}}. \tag{2.15}$$

The noncritical k_i are from Eq. (2.9). Criticality implies $(y_j^+)^2-(y_j^-)^2=1$. Note that the contributions of the critical rapidities to the energy (2.10) cancel out. Equation (2.15) implies that the Bethe quantum numbers of the critical pair must satisfy

$$|I_j+I_{j*}|=N/2. \tag{2.16}$$

The generalization of this solution to the case of s real critical pairs,

$$y_{j_l}^0 y_{j_l*}^0=1, \quad l=1,\ldots,s, \tag{2.17}$$

with Bethe quantum numbers satisfying $|I_{j_l}+I_{j_l*}|=N/2$ is straightforward. The noncritical rapidities are as in Eq. (2.9) and the critical pairs are determined from

$$\phi(y_{j_l}^-)=\frac{2}{N}\phi\left(\left[\frac{\sigma_{j_l}y_{j_l}^-}{1-\xi_{j_l}}\right]^{\sigma_{j_l}}\right), \quad l=1,\ldots,s \tag{2.18}$$

with ξ_{j_l},σ_{j_l} as defined in Eqs. (2.14) and (2.15).

C. Complex critical pairs

Next we consider the case of a single complex conjugate critical pair

$$y_1 = y_2^* = u + \mathrm{i}v \tag{2.19}$$

among the set of rapidities $y_1, \ldots, y_r$. Equations (2.6), rewritten as real equations, read

$$N\phi(c_2 y_i) = 2\pi I_i + \sum_{\substack{j=3 \\ j\neq i}}^{r} \phi\left(\frac{c_1(y_i - y_j)}{1 - y_i y_j}\right) + \phi\left(\frac{2c_1[(y_i-u)(1-y_i u) + y_i v^2]}{(1-y_i u)^2 + (y_i v)^2 - c_1^2[(y_i-u)^2 + v^2]}\right) \tag{2.20}$$

for $i = 3, \ldots, r$ and

$$N\phi\left(\frac{2c_2 u}{1 - c_2^2(u^2+v^2)}\right) = 2\pi(I_1 + I_2) + \sum_{i=3}^{r} [2\pi I_i - N\phi(c_2 y_i)], \tag{2.21}$$

$$N\varphi\left(\frac{2c_2 v}{1 + c_2^2(u^2+v^2)}\right) = \varphi\left(\frac{4v c_1(1-u^2-v^2)}{(1-u^2-v^2)^2 + (2v c_1)^2}\right) + \sum_{j=3}^{r} \varphi\left(\frac{2c_1 v(1-y_j^2)}{(1-y_j u)^2 + (y_j v)^2 + c_1^2[(y_j-u)^2 + v^2]}\right) \tag{2.22}$$

with $\varphi(x) \doteq 2\,\mathrm{atanh}(x)$ for the critical pair. The XX limit is performed along the path $u = u^0 - c_1 u^1$, $v = v^0 - c_1 v^1$. The only possible complex solutions that can survive the limit $c_1 \to 0$ are critical pairs. The noncritical roots are again as in Eq. (2.9). The critical pair of rapidities is now determined by the equation

$$\left(\frac{1+v^0}{1-v^0}\right)^N = \left(\frac{1-\xi_1+v^0}{1-\xi_1-v^0}\right)^2, \quad u_0^2 + v_0^2 = 1, \tag{2.23}$$

where

$$\xi_1 \equiv \frac{2}{N}\sum_{i=3}^{r} \frac{u^0 - \sin k_i}{(u^0)^{-1} - \sin k_i}, \tag{2.24}$$

$$\mathrm{sgn}\left(\frac{u_0}{\xi_1}\right) = -\frac{2}{N}(I_1 + I_2). \tag{2.25}$$

As is custom,[1] we shall replace $I_1 + I_2$ by a single Bethe quantum number $I^{(*)} \pm N/2$. We then have $I^{(*)} = 0$ for all complex critical pairs.

D. Generic case

Suppose we have t critical pairs of complex conjugate solutions, $y_1 = u_1 + iv_1 = y_2^*, \ldots, y_{2t-1} = u_t + iv_t = y_{2t}^*$, and s pairs of critical real solutions, $\mathcal{J}_l = \{j_l, j_l^*\} \subset \{2t+1, \ldots, r\}$, $l = 1, \ldots, s$. Then the real solutions in the limit $c_1 \to 0$ are of the form

$$y_i^0 = \tan\frac{\pi}{N} I_i, \quad i \notin \{1, \ldots, 2t\} \cup \bigcup_{l=1}^{s} \mathcal{J}_l, \tag{2.26}$$

$$\phi(y_{j_l}^-) = \frac{2}{N}\phi([\sigma_{j_l} y_{j_l}^- / (1 - \xi_{j_l})]^{\sigma_{j_l}}), \quad l = 1, \ldots, s, \tag{2.27}$$

with

$$\xi_{j_l} \doteq \frac{2}{N}\left[\sum_{\substack{i=2t+1 \\ i\neq j_l, j_l^*}}^{r} \frac{y_{j_l}^+ - \sin k_i^0}{y_{j_l}^{+-1} - \sin k_i^0} + 2\sum_{i=1}^{t} \frac{y_{j_l}^+ - (u_i^0)^{-1}}{y_{j_l}^{+-1} - (u_i^0)^{-1}}\right]. \tag{2.28}$$

For the complex solutions we obtain

$$\left(\frac{1+v_i^0}{1-v_i^0}\right)^N = \left(\frac{1-\xi_i+v_i^0}{1-\xi_i-v_i^0}\right)^2, \tag{2.29}$$

$$(u_i^0)^2 + (v_i^0)^2 = 1, \quad i = 1, \ldots, t, \tag{2.30}$$

with

$$\xi_i \doteq \frac{2}{N}\left[\sum_{j=2t+1}^{r} \frac{u_i^0 - \sin k_j^0}{u_i^{0-1} - \sin k_j^0} + 2\sum_{\substack{j=1 \\ j\neq i}}^{t} \frac{u_i^0 - (u_j^0)^{-1}}{(u_i^0)^{-1} - (u_j^0)^{-1}}\right]. \tag{2.31}$$

Energy and momentum of the state are determined by the noncritical roots alone:

$$E = -\sum_{\substack{i=2t+1 \\ i\neq j_1, \ldots, j_l^*}}^{r} \cos\left(\frac{2\pi}{N} I_i\right), \tag{2.32}$$

$$k = \pi(r - s - t) - \frac{2\pi}{N}\sum_{\substack{i=2t+1 \\ i\neq j_1, \ldots, j_l^*}}^{r} I_i (\mathrm{mod}\, 2\pi). \tag{2.33}$$

This prescription for handling Bethe ansatz solutions in the XX limit will guarantee that all XXZ Bethe eigenstates can be traced continuously across the point $\Delta = 0$. Because of the higher symmetry at $\Delta = 0$ and the associated level degeneracies,[12–14] the relationship between the (real and complex) Bethe eigenstates and the (always real) Jordan-Wigner eigenstates of the XX chain is nontrivial. The two representations will now be compared for all energy levels.

III. SPINONS VERSUS FERMIONS

The full spectrum of the XXZ model can be accounted for as composites of *interacting spinons* with spin 1/2 and semionic exclusion statistics.[22] For the XX case an alternative and

TABLE I. Dimensionalities $W(n_+,n_-)$ of the invariant subspaces with $2n$ spinons and spin $S_T^z=n_+-n_-$ for a chain of length $N=8$. The equivalent quantum numbers in the fermion representation are $N_f=N/2-S_T^z$, $n_c=n-|S_T^z|$.

n_+-n_-	$n=0$	$n=1$	$n=2$	$n=3$	$n=4$	$\Sigma_n W$
8				1		1
6				7	1	8
4			15	12	1	28
2		10	30	15	1	56
0	1	16	36	16	1	70
−2		10	30	15	1	56
−4			15	12	1	28
−6				7	1	8
−8					1	1
$\Sigma_{n_+} W$	1	36	126	84	9	256

equivalent interpretation of the complete spectrum can be established on the basis of *noninteracting spinless lattice fermions*. How are spinon configurations related to fermion configurations in single nondegenerate eigenstates and in groups of degenerate eigenstates?

Consider the 2^N-dimensional Hilbert space for even N divided into subspaces characterized by n_+ spinons with spin up and n_- spinons with spin down. Equivalent quantum numbers are the total number of spinons and the z component of the total spin:

$$2n=n_++n_-, \quad 2S_T^z=n_+-n_-. \tag{3.1}$$

The dimensionality of each such subspace is[22]

$$W(n_+,n_-)=\prod_\sigma \binom{d_\sigma+n_\sigma-1}{n_\sigma}, \tag{3.2}$$

$$d_\sigma=\tfrac{1}{2}(N+1)-\tfrac{1}{2}\sum_{\sigma'}(n_{\sigma'}-\delta_{\sigma\sigma'}), \tag{3.3}$$

where $\sigma=\pm$ denotes the spinon polarization. Summing $W(n_+,2n-n_+)$ over n or n_+ yields

$$\sum_{n=1}^{N/2} W=\binom{N}{n_+}, \quad \sum_{n_+=0}^{2n} W=\binom{N+1}{2n}, \tag{3.4}$$

respectively. The double sum yields 2^N. In Table I we list the subspace dimensionalities for the case $N=8$.

The XX Hamiltonian in the fermion representation, transformed from Eq. (1.1) at $\Delta=0$ by the Jordan-Wigner mapping to a system of free spinless fermions, reads[23]

$$H_f=\sum_p \cos p\, c_p^\dagger c_p, \tag{3.5}$$

where the allowed values of the fermion momenta p_i depend on whether the number N_f of fermions in the system is even or odd:

$$p_i\in\{(2\pi/N)(n+1/2)\} \quad (N_f \text{ even}), \tag{3.6a}$$

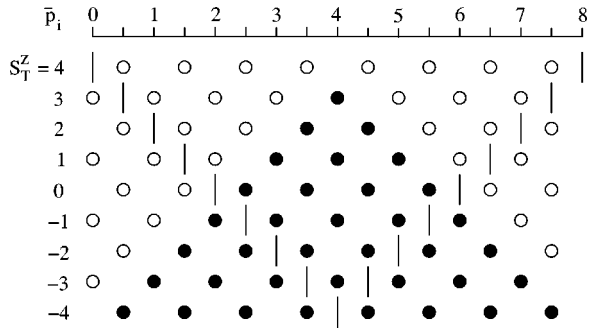

FIG. 1. Configuration in reciprocal space of the $N_f=N/2-S_T^z$ fermions in the lowest-energy eigenstate for given S_T^z of a chain with $N=8$ spins. The positions of the fermions are denoted by full circles, and those of vacancies by open circles. The fermion momenta $\bar{p}_i$ are in units of $2\pi/N$. The vertical bars are at wave numbers (also in units of $2\pi/N$) $\bar{k}_c^-=N/4-S_T^z/2$ and $\bar{k}_c^+=3N/4+S_T^z/2$.

$$p_i\in\{(2\pi/N)n\} \quad (N_f \text{ odd}), \tag{3.6b}$$

for $n=0,1,\ldots,N-1$. The number of fermions ($0\leqslant N_f\leqslant N$) is related to the quantum number S_T^z in the spin representation: $S_T^z=N/2-N_f$. No matter whether N_f is even or odd, there are N distinct one-particle states. Every one-particle state can be either empty or singly occupied, yielding a total of 2^N distinct many-particle states with energy and wave number

$$E-E_F=\sum_{i=1}^{N_f}\cos p_i, \quad k=\sum_{i=1}^{N_f} p_i. \tag{3.7}$$

The lowest-energy state in each S_T^z subspace is unique. The fermion configuration in reciprocal space of each lowest-energy state for $N=8$ is shown in Fig. 1.

For the further subdivision of each S_T^z subspace, we introduce the wave numbers

$$\frac{k_c^\pm}{\pi}=1\pm\left(\frac{1}{2}+\frac{S_T^z}{N}\right) \tag{3.8}$$

shown as vertical bars in Fig. 1, dividing the band into two regions, one in the center and the other in the wings. Given that the lowest-energy state at $S_T^z\geqslant 0$ has all particles in the center region, we can characterize all excitations as n_c-particle states. Likewise, all excitations from the lowest-energy state at $S_T^z\leqslant 0$ can be characterized as n_c-hole states. The range of this second quantum number is $n_c=0,1,\ldots,N/2-|S_T^z|$. The number of fermion states characterized by n_c particles or n_c holes in the above sense is then found to be as expression (3.2) previously used for spinons, now with

$$n=n_c+|S_T^z|, \quad n_\pm=n_c+|S_T^z|\pm S_T^z. \tag{3.9}$$

The next goal is to bring the mapping down to energy levels (at fixed wave numbers) within each (n_+,n_-) subspace or, in the fermion language, (S_T^z,n_c) subspace.[24] We note that for given $S_T^z\geqslant 0$ the number of fermions is equal to

the number of magnons in Bethe ansatz states. Moreover, the fermion energy-momentum relation (3.7) is equivalent to the magnon energy-momentum relation (2.10). The exception are the critical magnon pairs, whose momenta are different (real or complex) from the corresponding fermion momenta (always real). Critical pairs only occur in degenerate levels and do not contribute to the energy of the state.

This mapping between energy levels provides a useful tool for determining the Bethe quantum numbers of eigenstates directly from the momenta of the fermion configurations. For all noncritical rapidities, we have

$$\frac{2\pi}{N} I_i = \pi - p_i . \tag{3.10}$$

For real critical pairs, the Bethe quantum numbers are, in general, shifted relative to the positions predicted by Eq. (3.10), but in such a way $|I_j + I_{j*}| = N/2$ is maintained. Complex critical pairs are specified by a single Bethe quantum number $I^{(*)} = 0$ as discussed in Sec. II C. In the following, we look more closely at the two-spinon excitations in the two representations.

IV. TWO-SPINON SPECTRUM

A. Planar *XXZ* model

Returning to the *XXZ* model (1.1), we note that there exist two-spinon states with $S_T^z = 0, \pm 1$. At $\Delta = 1$ these states are either triplets (with total spin $S_T = 1$) or singlets ($S_T = 0$). There are $\frac{1}{8}N(N+2)$ triplet levels and $\frac{1}{8}N(N-2)$ singlet levels, distinguishable by their Bethe quantum numbers.[17,25] Integrability guarantees that each eigenstate anywhere in the planar regime can be traced back to the point of higher symmetry without ambiguity. This justifies that we use the S_T multiplet labels for states at $\Delta < 1$.

At finite N and $\Delta < 1$, the two-spinon triplet components with $S_T^z = \pm 1$ remain degenerate (because of reflection symmetry in spin space) but are no longer degenerate with the two-spinon triplet components with $S_T^z = 0$. We shall see that at $\Delta = 0$, a subset of $\frac{1}{8}N(N-2)$ states from the latter set becomes degenerate with the two-spinon singlets.

We have tracked the Bethe ansatz solutions of every two-spinon state for $N = 8$ from $\Delta = 1$ to $\Delta = 0$, indeed across this highly singular point of the Bethe ansatz equations all the way to $\Delta = -1$. Here we briefly report on what we found along the stretch $0 < \Delta < 1$.[26] For all states, solutions of the Bethe ansatz equations were found for which all magnon momenta k_i (or all rapidities y_i) vary continuously across the parameter regime.

The two-spinon triplets with $S_T^z = 1$ are easy to handle numerically. All rapidities y_i are finite and real. Two-spinon triplets with $S_T^z = 0$, by contrast, tend to pose some computational challenges. At $\Delta = 1$ all such states start out with one $k_i = 0$ magnon, implying $y_i = \pm\infty$. While this singular behavior is benign,[17] numerical problems are caused by the fact that in some states y_i stays infinite at $\Delta < 1$, whereas in other states it becomes finite. The majority of states from this set have one real critical pair at $\Delta = 0$. Toensure continuity of the Bethe ansatz solutions when $\Delta$is varied, it is sometimes necessary to change the values of two Bethe quantum numbers leaving their sum invariant.

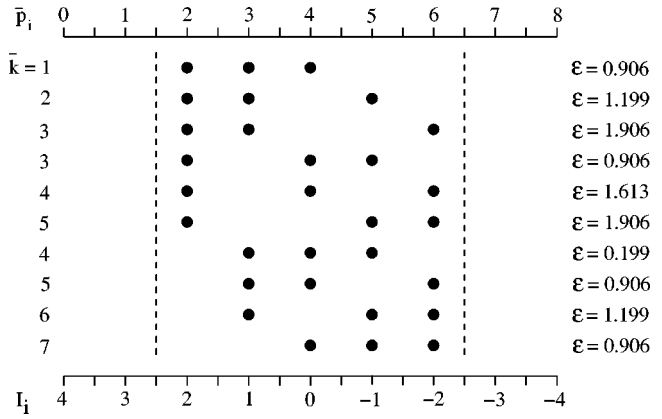

FIG. 2. Set of $N(N+2)/8$ two-spinon states with $S_T^z = 1$ at $\Delta = 0$ for $N = 8$ as specified by the fermion momenta (top scale) or Bethe quantum numbers (bottom scale). The wave numbers $\bar{k}$ and fermion momenta $\bar{p}_i$ are in units of $2\pi/N$. The dashed lines represent $\bar{k}_c^-$ and $\bar{k}_c^+$. The energies are $\epsilon = E - E_G$ relative to the ground state with $E_G = -2.613$.

The two-spinon singlets are far more difficult to handle numerically. Each such state has one complex-conjugate pair of rapidities. A numerical analysis of two-spinon singlets at $\Delta = 1$ was reported in Ref. 17. Again, continuity of the solutions may make it necessary to change some Bethe quantum numbers along the way. At $\Delta = 0$ each state from this set with one complex-conjugate critical pair becomes degenerate with a two-spinon triplet state that has one real critical pair.

B. *XX* limit

According to the scheme developed in Sec. III, the two-spinon states with $S_T^z = 1$ comprise all configurations in which no state with positive energy in the fermion band is occupied. These are the fermion configurations with $n_c = 0$. The $N/2+1$ single-particle states which are accessible under this restriction and among which the $N/2-1$ fermions can be distributed do indeed produce $N(N+2)/8$ distinct eigenstates. All possible configurations for $N = 8$, generated systematically across the allowed range in reciprocal space, are depicted in Fig. 2.

No critical pairs can be formed in any of these states, which makes it straightforward to calculate transition rates for fairly long chains (see Sec. VI).

The two-spinon states with $S_T^z = 0$ comprise all ($n_c = 1$) states relative to the ground-state configuration in the fermion band. Removing one of $N/2$ fermions from the ground-state configuration and placing it into one of the $N/2$ empty single-particle states yields $N^2/4$ distinct eigenstates but only $N(N+2)/8$ distinct levels in the (k,E) plane because of degeneracies. All possible configurations for $N = 8$ including the ground state, generated systematically across the allowed range in reciprocal space, are depicted as rows of full circles in Fig. 3.

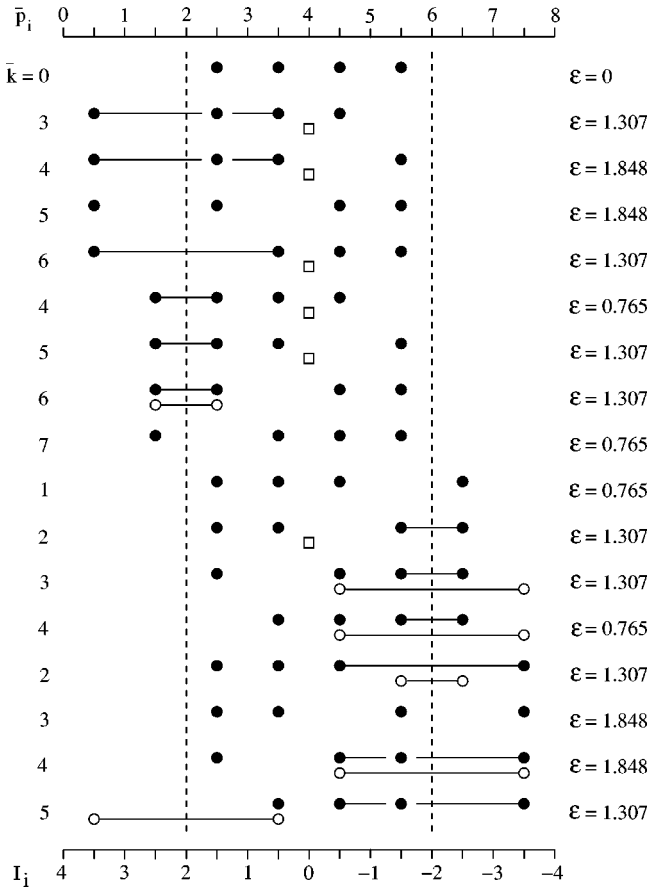

FIG. 3. Ground state and set of $N^2/4=N(N+2)/8+N(N-2)/8$ two-spinon states with $S_T^z=0$ for $N=8$. The positions of the full circles in relation to the top scale denote the fermion momenta and those in relation to the bottom scale the Bethe quantum numbers predicted via Eq. (3.10). The critical pairs among them are connected by a solid line. The open circles and squares denote the actual Bethe quantum numbers associated with the critical pairs for real and complex rapidities, respectively. The wave numbers $\bar{k}$ and fermion momenta $\bar{p_i}$ are in units of $2\pi/N$. The dashed lines represent $\bar{k_c^-}$ and $\bar{k_c^+}$.

There are $N(N-2)/8$ twofold degenerate levels in the (k,E) plane with the two states distinguished by one pair of fermions. The two fermions in question (full circles connected by a line in Fig. 3) add up to $\pi \mathrm{mod}(2\pi)$, thus contributing nothing to the energy (3.7). Additionally, there exist $N/2$ nondegenerate ($n_c=1$) states at wave numbers $Nk/2\pi=1,3,\ldots,N-1$ representing the highest-energy two-spinon state for those wave numbers.

In summary, the $N^2/4$ ($n_c=1$) states in the fermion representation at $\Delta=0$ originate from the set of $N(N+2)/8$ two-spinon triplets with $S_T^z=0$ and the set of $N(N-2)/8$ two-spinon singlets. Each singlet becomes degenerate with a triplet at $\Delta=0$, while $N/2$ triplets remain nondegenerate. When analyzed via Bethe ansatz, the two states of each degenerate two-spinon level with $S_T^z=0$ have one critical pair of magnon momenta as described in Sec. II. Our analysis shows that the critical pair is real for the triplet state and complex for the singlet state. This is consistent with the known two-string nature of the two-spinon singlets and one-string nature of the two-spinon triplets at $\Delta=1$.

In the states with real critical pairs, a solution may only exist for Bethe quantum numbers that are shifted relative to those predicted by Eq. (3.10) but still satisfy Eq. (2.16). The latter are indicated in Fig. 3 by open circles. In states with complex conjugate critical pairs, two of the Bethe quantum numbers (3.10) are replaced by a single number $I^{(*)}=0$ representing the critical pair.

The actual Bethe ansatz solutions for $N=8$ pertaining to all $N^2/4$ two-spinon states with $S_T^z=0$ are listed in Table II (triplets) and Table III (singlets). In some instances, different configurations of Bethe quantum numbers lead to equivalent Bethe wave functions. Only one configuration is represented in Fig. 3.[27]

V. MATRIX ELEMENTS VIA BETHE ANSATZ FOR $\Delta=0$

We start from the determinantal expressions for the transition rates

TABLE II. Wave number, energy, magnon momenta, Bethe quantum numbers, and rapidities of the $N(N+2)/8$ two-spinon triplet components with $S_T^z=0$ at $\Delta=0$ for $N=8$. The quantities $\bar{k},\bar{k_i}$ are in units of $2\pi/N$.

$\bar{k}$	$E-E_G$	$\bar{k_1}$	$\bar{k_2}$	$\bar{k_3}$	$\bar{k_4}$	I_1	I_2	I_3	I_4	y_1	y_2	y_3	y_4
0	0.000	2.5	3.5	4.5	5.5	1.5	0.5	−0.5	−1.5	0.668	0.199	−0.199	−0.668
1	0.765	2.5	3.5	4.5	6.5	1.5	0.5	−0.5	−2.5	0.668	0.199	−0.199	−1.497
2	1.307	2.5	3.5	5.110	6.890	1.5	0.5	−1.5	−2.5	0.668	0.199	−0.466	−2.147
3	1.307	2.5	4.5	4.728	7.272	1.5	−0.5	−0.5	−3.5	0.668	−0.199	−0.294	−3.402
	1.848	2.5	3.5	5.5	7.5	1.5	0.5	−1.5	−3.5	0.668	0.199	−0.668	−5.027
4	0.765	3.5	4	4.5	0	0.5	−0.5	−0.5	−3.5	0.199	0	−0.199	−∞
	1.848	2.5	4	5.5	0	1.5	−0.5	−1.5	−3.5	0.668	0	−0.668	−∞
5	1.307	0.728	3.272	3.5	5.5	3.5	0.5	0.5	−1.5	3.402	0.294	0.199	−0.668
	1.848	0.5	2.5	4.5	5.5	3.5	1.5	−0.5	−1.5	5.027	0.668	−0.199	−0.668
6	1.307	1.110	2.890	4.5	5.5	2.5	1.5	−0.5	−1.5	2.147	0.466	−0.199	−0.668
7	0.765	1.5	3.5	4.5	5.5	2.5	0.5	−0.5	−1.5	1.497	0.199	−0.199	−0.668

TABLE III. Wave number, energy, magnon momenta, Bethe quantum numbers, and rapidities of the $N(N-2)/8$ two-spinon singlets at $\Delta=0$ for $N=8$. The quantities $\bar{k},\bar{k}_i$ are in units of $2\pi/N$.

$\bar{k}$	$E-E_G$	$\bar{k}^*$	$\bar{k}_3$	$\bar{k}_4$	$I^{(*)}$	I_3	I_4	u	v	y_3	y_4
2	1.307	4	3.5	2.5	0	0.5	1.5	−0.765	−0.644	0.199	0.668
3	1.307	4	4.5	2.5	0	−0.5	1.5	−0.541	−0.841	−0.199	0.668
4	0.765	4	4.5	3.5	0	−0.5	0.5	0	1	−0.199	0.199
	1.848	4	5.5	2.5	0	−1.5	1.5	0	1	−0.668	0.668
5	1.307	4	5.5	3.5	0	−1.5	0.5	0.541	0.841	−0.668	0.199
6	1.307	4	5.5	4.5	0	−1.5	−0.5	0.765	0.644	−0.668	−0.199

$$M_\lambda^\mu(q)\doteq\frac{|\langle\psi_0|S_q^\mu|\psi_\lambda\rangle|^2}{\|\psi_0\|^2\|\psi_\lambda\|^2},\quad \mu=z,+,-, \tag{5.1}$$

between XXZ eigenstates characterized by real k_i for the spin operators

$$S_q^\mu=\frac{1}{\sqrt{N}}\sum_n e^{iqn}S_n^\mu,\quad \mu=z,+,-. \tag{5.2}$$

These expressions, which were derived in Ref. 10 based on previous work reported in Refs. 6–8, have the form

$$M_\lambda^z(q)=\frac{N}{4}\frac{\mathcal{K}_r(\{y_i^0\})}{\mathcal{K}_r(\{y_i\})}\frac{\left|\det\left(\Gamma-\frac{2}{N}1\right)\right|^2}{\det\mathsf{K}(\{y_i^0\})\det\mathsf{K}(\{y_i\})}, \tag{5.3}$$

$$M_\lambda^\pm(q)=\left(\frac{\mathcal{K}_{r\pm1}(\{y_i\})}{\mathcal{K}_r(\{y_i^0\})}\right)^{\pm1}\frac{|\det\Gamma^\pm|^2}{\det\mathsf{K}(\{y_i\})\det\mathsf{K}(\{y_i^0\})}, \tag{5.4}$$

where

$$\mathsf{K}_{ab}=\begin{cases}\dfrac{\cos\gamma}{N}\dfrac{K(y_a,y_b)}{\kappa(y_a)}, & a\neq b\\[2ex] 1-\dfrac{\cos\gamma}{N}\displaystyle\sum_{j\neq a}^{r}\frac{K(y_a,y_j)}{\kappa(y_a)}, & a=b,\end{cases} \tag{5.5}$$

$$\Gamma_{ab}\doteq F_N(y_a^0,y_b)\left(\frac{1}{G(y_a^0,y_b)}\prod_{j=1}^{r}\frac{G(y_j^0,y_b)}{G(y_j,y_b)}+\frac{1}{G^*(y_a^0,y_b)}\prod_{j=1}^{r}\frac{G^*(y_j^0,y_b)}{G^*(y_j,y_b)}\right), \tag{5.6}$$

$$\Gamma_{ab}^+\doteq F_N(y_a,y_b^0)\left(\frac{G(y_{r+1},y_b^0)}{G(y_a,y_b^0)}\prod_{j=1}^{r}\frac{G(y_j,y_b^0)}{G(y_j^0,y_b^0)}+\frac{G^*(y_{r+1},y_b^0)}{G^*(y_a,y_b^0)}\prod_{j=1}^{r}\frac{G^*(y_j,y_b^0)}{G^*(y_j^0,y_b^0)}\right),$$

$$\Gamma_{a,r+1}^+\doteq 1,\ a=1,\ldots,r+1,\ b=1,\ldots,r,$$

$$\Gamma_{ab}^-\doteq F_N(y_a^0,y_b)\left(\frac{G(y_r^0,y_b)}{G(y_a^0,y_b)}\prod_{j=1}^{r-1}\frac{G(y_j^0,y_b)}{G(y_j,y_b)}+\frac{G^*(y_r^0,y_b)}{G^*(y_a^0,y_b)}\prod_{j=1}^{r-1}\frac{G^*(y_j^0,y_b)}{G^*(y_j,y_b)}\right), \tag{5.7}$$

$$\Gamma_{ar}^-\doteq 1,\quad a=1,\ldots,r,\quad b=1,\ldots,r-1, \tag{5.8}$$

$$\mathcal{K}_r(\{y_i\})\doteq\prod_{i<j}^{r}|K(y_i,y_j)|, \tag{5.9}$$

$$K(y,y')\doteq\frac{(1-y^2)(1-y'^2)\sin^2\gamma}{(y-y')^2+(1-y^2)(1-y'^2)\sin^2\gamma}, \tag{5.10}$$

$$\kappa(y)\doteq\frac{(y^{-1}-y)\sin\gamma}{y\cot(\gamma/2)+[y\cot(\gamma/2)]^{-1}}, \tag{5.11}$$

$$G(y,y')\doteq\frac{(y-y')\cot\gamma+i(1-yy')}{\sqrt{1-y^2}\sqrt{1-y'^2}}, \tag{5.12}$$

$$F_N(y,y')\doteq\frac{1}{2N}\frac{\sqrt{1-y'^2}}{\sqrt{1-y^2}}\frac{1+y^2+(y^2-1)\cos\gamma}{(y-y')\sin\gamma}. \tag{5.13}$$

Performing the XX limit, $\gamma\to\pi/2$, in these expressions is straightforward as long as no critical pairs of rapidities are present:

$$K(y,y')=\frac{(1-y^2)(1-y'^2)}{(1-yy')^2}, \tag{5.14}$$

$$\kappa(y)=\frac{y^{-1}-y}{y^{-1}+y}, \tag{5.15}$$

$$G(y,y')=i\frac{1-yy'}{\sqrt{1-y^2}\sqrt{1-y'^2}}, \tag{5.16}$$

$$F_N(y,y')=\frac{1}{2N}\frac{\sqrt{1-y'^2}}{\sqrt{1-y^2}}\frac{1+y^2}{y-y'}, \tag{5.17}$$

$$\det\mathsf{K}=1. \tag{5.18}$$

Switching back from the noncritical rapidities via Eq. (2.9), $y_i = \cot(k_i/2)$, to the noncritical magnon momenta k_i, we can bring expression (5.4) into the form

$$M_\lambda^+(q) = \frac{\prod_{i=1}^{r}\prod_{j=1}^{r+1}\cos^2\frac{k_i^0+k_j}{2}}{\prod_{i<j}^{r+1}\cos^2\frac{k_i+k_j}{2}\prod_{i<j}^{r}\cos^2\frac{k_i^0+k_j^0}{2}}|\det\mathcal{S}^+|^2,$$

$$\mathcal{S}_{ab}^+ \doteq \begin{cases} \dfrac{2/N}{\sin k_a - \sin k_b^0}, & b=1,\ldots,r \\ 1, & b=r+1 \end{cases}, \quad a=1,\ldots,r+1,$$

$$M_\lambda^-(q) = \frac{\prod_{i=1}^{r}\prod_{j=1}^{r-1}\cos^2\frac{k_i^0+k_j}{2}}{\prod_{i<j}^{r-1}\cos^2\frac{k_i+k_j}{2}\prod_{i<j}^{r}\cos^2\frac{k_i^0+k_j^0}{2}}|\det\mathcal{S}^-|^2, \tag{5.19}$$

$$\mathcal{S}_{ab}^- \doteq \begin{cases} \dfrac{2/N}{\sin k_a^0 - \sin k_b}, & b=1,\ldots,r-1 \\ 1, & b=r \end{cases} \quad a=1,\ldots,r, \tag{5.20}$$

where $\mathcal{S}^\pm$ are Cauchy-type matrices, whose determinants can be evaluated explicitly:

$$\det\mathcal{S}^+ = \left(\frac{2}{N}\right)^r \frac{\prod_{i<j}^{r}(\sin k_i^0 - \sin k_j^0)\prod_{i<j}^{r+1}(\sin k_j - \sin k_i)}{\prod_{i=1}^{r}\prod_{j=1}^{r+1}(\sin k_j - \sin k_i^0)},$$

$$\det\mathcal{S}^- = \left(\frac{2}{N}\right)^{r-1} \frac{\prod_{i<j}^{r}(\sin k_j^0 - \sin k_i^0)\prod_{i<j}^{r-1}(\sin k_i - \sin k_j)}{\prod_{i=1}^{r}\prod_{j=1}^{r-1}(\sin k_i^0 - \sin k_j)}.$$

This reduces the transition rates for the perpendicular spin fluctuations (between states without critical pairs) to compact product expressions:

$$M_\lambda^+(q) = \frac{\prod_{i<j}^{r+1}\sin^2\frac{k_i-k_j}{2}\prod_{i<j}^{r}\sin^2\frac{k_i^0-k_j^0}{2}}{\prod_{i=1}^{r}N^2\prod_{j=1}^{r+1}\sin^2\frac{k_i^0-k_j}{2}}, \tag{5.21}$$

$$M_\lambda^-(q) = \frac{\prod_{i<j}^{r-1}\sin^2\frac{k_i-k_j}{2}\prod_{i<j}^{r}\sin^2\frac{k_i^0-k_j^0}{2}}{\prod_{j=1}^{r-1}N^2\prod_{i=1}^{r}\sin^2\frac{k_i^0-k_j}{2}}. \tag{5.22}$$

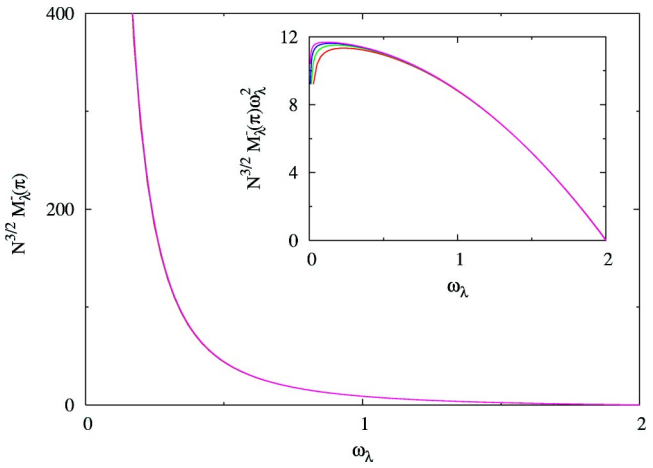

FIG. 4. Scaled two-spinon transition rates $\bar{M}_{-+}^{(2)}(\pi,\omega) = N^{3/2}M_\lambda^-(\pi)$ at $\Delta=0$ (data for chains of size $N=512,1024,2048,4096$). The inset shows the same quantity multiplied by ω_λ^2.

In the corresponding reduction of the transition rate (5.3) for the parallel spin fluctuations, a complication arises, caused by the possibility that some magnon momenta of the two states might be identical. However, this singular behavior turns out to be instrumental for the exact evaluation of $M_\lambda^z(q)$. A nonzero result is only possible if the two sets of Bethe quantum numbers $\{I_i^{(0)}\}$ and $\{I_i\}$ differ by no more than one element. For all such transitions the rate is

$$M_\lambda^z(q) = \frac{1}{N}, \tag{5.23}$$

in agreement with a well-known result derived in the fermion representation.[28]

In the following application of the transition rate expressions to a $T=0$ spin dynamic structure factor of the XX model we have chosen a situation where excited states without critical rapidities are important. The calculation of transition rates with critical pairs requires further developmental work.

VI. TWO-SPINON TRANSITION RATES

From recent studies in the framework of the algebraic analysis for the infinite chain,[29,30] we know that the relative integrated intensity of the two-spinon contribution to the dynamic structure factor

$$S_{-+}(q,\omega) = 2\pi\sum_\lambda M_\lambda^-(q)\,\delta(\omega-\omega_\lambda) \tag{6.1}$$

probing the spin fluctuations perpendicular to the symmetry axis of the XXZ model is 73% for the Heisenberg case ($\Delta=1$) and steadily growing toward 100% on approach of the Ising case ($\Delta=\infty$).

The nonzero two-spinon intensity is reflected in the reciprocal finite-N scaling behavior of the transition rates $M_{-+}^{(2)}(q,\omega_\lambda) = NM_\lambda^-(q)$ and the scaled density of states

$$D^{(2)}(q,\omega_\lambda)=2\pi/[N(\omega_{\lambda+1}-\omega_\lambda)], \tag{6.2}$$

which makes the product

$$S^{(2)}_{-+}(q,\omega)=M^{(2)}_{-+}(q,\omega)D^{(2)}(q,\omega) \tag{6.3}$$

converge toward a piecewise smooth function in the limit $N\to\infty$, representing the result of the infinite chain.

A qualitatively different finite-N scaling behavior is found in the XX case ($\Delta=0$) for the two-spinon transition rates contributing to $S_{-+}(q,\omega)$. For the transition rates to converge toward a nonvanishing piecewise smooth function they must be scaled differently: $\overline{M}^{(2)}_{-+}(q,\omega)=N^{3/2}M^-_\lambda(q)$. This is illustrated in Fig. 4 for $q=\pi$. In the main plot we show data for $N=512,1024,2048,4096$ of $N^{3/2}M^-_\lambda(\pi)$ versus ω_λ. The scaling is near perfect across the band. The divergence building up as $N\to\infty$ in this quantity is stronger, $\sim\omega^{-2}$, than the known infrared singularity in the dynamic structure factor,[31] $S_{-+}(q,\omega)\sim\omega^{-3/2}$, as documented by the inset to Fig. 4.

Given the nonreciprocal scaling behavior of the transition rates and density of states, the relative intensity of the two-spinon dynamic structure factor $S^{(2)}_{-+}(q,\omega)$ vanishes in the limit $N\to\infty$. Hence the singularity structure of the function $\overline{M}^{(2)}_{-+}(q,\omega)$ has no direct bearing on the singularity structure of $S_{-+}(q,\omega)$. A distinct singularity structure and spectral-weight distribution which is a property of all $2m$-spinon excitations combined will emerge in the limit $N\to\infty$.

Consequently, the exactly known leading singularities at $\omega=0,1,2,\ldots$ in the frequency-dependent spin autocorrelation function $\Phi_0^{-+}(\omega)=\int_{-\pi}^{+\pi}(dq/2\pi)S_{-+}(q,\omega)$, as worked out in Ref. 32, for example, are not attributable to specific $2m$-fermion excitations, because the integrated intensity of each $2m$-fermion contribution taken in isolation is likely to vanish in the limit $N\to\infty$.

To reconstruct the spectral-weight distribution of $S_{-+}(q,\omega)$ at $\Delta=0$ and to determine its singularity structure in the limit $N\to\infty$ from finite-N data for excitation energies and transition rates we need to be able to properly handle Bethe wave functions with critical pairs of rapidities. We already know (Sec. II) how to solve the Bethe ansatz equations for all eigenstates in the limit $\Delta\to0$. One challenging problem for the calculation of transition rates is that Bethe wave functions with critical pairs thus obtained vanish identically as pointed out in Ref. 33. However, our numerical analysis strongly suggests that the vanishing norm $\|\psi_\lambda\|$ in the denominator of Eq. (5.1) is compensated by the vanishing transition rate in the numerator to produce a unique finite ratio in the limit $\Delta\to0$.[34]

[1] M. Takahashi, *Thermodynamics of One-Dimensional Solvable Models* (Cambridge University Press, Cambridge, UK, 1999).

[2] V.E. Korepin, N.M. Bogoliubov, and A.G. Izergin, *Quantum Inverse Scattering Method and Correlation Functions* (Cambridge University Press, Cambridge, 1993).

[3] M. Karbach and G. Müller, Phys. Rev. B **62**, 14 871 (2000).

[4] M. Karbach, D. Biegel, and G. Müller, Phys. Rev. B **66**, 054405 (2002).

[5] Throughout this paper, the exchange constant is used as energy unit: $J=1$.

[6] V.E. Korepin, Commun. Math. Phys. **86**, 391 (1982).

[7] A.G. Izergin and V.E. Korepin, Commun. Math. Phys. **99**, 271 (1985).

[8] N. Kitanine, J.M. Maillet, and V. Terras, Nucl. Phys. B **554**, 647 (1999).

[9] D. Biegel, M. Karbach, and G. Müller, Europhys. Lett. **59**, 882 (2002).

[10] D. Biegel, M. Karbach, and G. Müller, J. Phys. A **36**, 5361 (2003).

[11] J. des Cloizeaux and M. Gaudin, J. Math. Phys. **7**, 1384 (1966).

[12] T. Deguchi, K. Fabricius, and B.M. McCoy, J. Stat. Phys. **102**, 701 (2001).

[13] K. Fabricius and B.M. McCoy, J. Stat. Phys. **103**, 647 (2001).

[14] K. Fabricius and B.M. McCoy, J. Stat. Phys. **104**, 573 (2001).

[15] The commonly used rapidities are $z_i=2\mathrm{atanh}y_i$. There exist Bethe ansatz solutions with real magnon momenta k_i for which $|\tanh(z_i/2)|>1$. Whereas some z_i thus become imaginary, all y_i stay real. Using the latter significantly facilitates the tasks of solving the Bethe ansatz equations and calculating transition rates.

[16] F.H.L. Essler, V.E. Korepin, and K. Schoutens, J. Phys. A **25**, 4115 (1992).

[17] M. Karbach, K. Hu, and G. Müller, Comput. Phys. **12**, 565 (1998).

[18] F. Woynarovich, J. Phys. C **15**, 6397 (1982).

[19] A.A. Vladimirov, Phys. Lett. **105A**, 418 (1984).

[20] K. Iseler and M. Paranjape, Phys. Lett. B **319**, 209 (1993).

[21] A. Ilakovac, M. Kolanovic, S. Pallua, and P. Prester, Phys. Rev. B **60**, 7271 (1999).

[22] F.D.M. Haldane, Phys. Rev. Lett. **67**, 937 (1991).

[23] E. Lieb, T. Schulz, and D. Mattis, Ann. Phys. (N.Y.) **16**, 407 (1961).

[24] A one-to-one mapping between individual states is not possible for degenerate levels because of the different natural eigenbases in the two representations.

[25] L.D. Faddeev and L.A. Takhtajan, Phys. Lett. **85A**, 375 (1981).

[26] D. Biegel, Diplomarbeit, Bergische Universität Gesamthochchule Wuppertal, 2000.

[27] Alternative sets of Bethe quantum numbers for the two states with $\overline{k}=4$ in Table III are $(3.5,0.5,0.5,-0.5)$ and $(3.5,1.5,0.5,-1.5)$, respectively.

[28] S. Katsura, T. Horiguchi, and M. Suzuki, Physica (Amsterdam) **46**, 67 (1970).

[29] M. Karbach, G. Müller, A.H. Bougourzi, A. Fledderjohann, and K.-H. Mütter, Phys. Rev. B **55**, 12 510 (1997).

[30] A.H. Bougourzi, M. Karbach, and G. Müller, Phys. Rev. B **57**, 11 429 (1998).

[31] A. Luther and I. Peschel, Phys. Rev. B **12**, 3908 (1975).

[32] G. Müller and R.E. Shrock, Phys. Rev. B **29**, 288 (1984).

[33] K. Fabricius and B.M. McCoy, J. Stat. Phys. **111**, 323 (2003).

[34] D. Biegel, M. Karbach, G. Müller, and K. Wiele (unpublished).